Vibrational Energy Transfer between Carbon Nanotubes and Nonaqueous Solvents: A Molecular Dynamics Study

ARTICLE *in* THE JOURNAL OF PHYSICAL CHEMISTRY B · NOVEMBER 2010

Impact Factor: 3.3 · DOI: 10.1021/jp108776q · Source: PubMed

4 AUTHORS, INCLUDING:

Tammie R. Nelson
Los Alamos National Laboratory
22 PUBLICATIONS **446** CITATIONS
SEE PROFILE

Victor Prezhdo
University of Rochester
26 PUBLICATIONS **312** CITATIONS
SEE PROFILE

Oleg Prezhdo
University of Rochester
306 PUBLICATIONS **6,774** CITATIONS
SEE PROFILE

THE JOURNAL OF PHYSICAL CHEMISTRY B

ARTICLE

pubs.acs.org/JPCB

Vibrational Energy Transfer between Carbon Nanotubes and Nonaqueous Solvents: A Molecular Dynamics Study

Tammie R. Nelson,[‖] Vitaly V. Chaban,[‡] Victor V. Prezhdo,[§] and Oleg V. Prezhdo*[,‡]

[‖]Department of Chemistry, University of Washington, Seattle, Washington 98195, United States

[‡]Department of Chemistry, University of Rochester, Rochester, New York 14627, United States

[§]Institute of Chemistry, Jan Kochanowski University, 25-406 Kielce, Poland

ABSTRACT: We report molecular dynamics (MD) simulation of energy exchange between single-walled carbon nanotubes (CNTs) and two aprotic solvents, acetonitrile and cyclohexane. Following our earlier study of hydrated CNTs, we find that the time scales and molecular mechanisms of the energy transfer are largely independent of the nature of the surrounding medium, and therefore, should hold for other media including polymer matrices and DNA. The vibrational energy exchange between CNT and solvents exhibits two time-scales. Over half of the energy is transferred in less than one picosecond, indicating that the dominant exchange mechanism is inertial relaxation. It occurs by collisions of solvent molecules with CNT walls, facilitated by the short-range Lennard-Jones interaction. Additional several picoseconds are required for the remainder of the vibrational energy exchange, corresponding to the diffusive relaxation mechanism and involving collective molecular motions. The faster stage of the CNT-solvent energy exchange occurs on the same time-scale, and therefore, competes with the vibrational energy relaxation inside CNTs. The energy exchange time-scales are significantly influenced by the arrangement of solvent molecules inside CNTs. Generally, the effects of confinement on the dynamics can be rationalized by analysis of the solvent structure. For the same CNT diameter, the extent of the confinement effect strongly depends on the size of the solvent molecules. Icelike properties in water seen in small CNTs disappear in CNTs with intermediate diameters. In acetonitrile and cyclohexane, medium size CNTs still show strong confinement effects. Rotational motions of acetonitrile molecules are inhibited, and the cyclohexane density is dramatically decreased. The disbalance between the local temperatures of the inside and outside regions of the solvent equilibrates through a tube-mediated interaction, rather than by a direct coupling between the two solvent subsystems. In all cases, the CNT-solvent energy transfer is mediated by slow motions in the frequency range of CNT radial breathing modes.

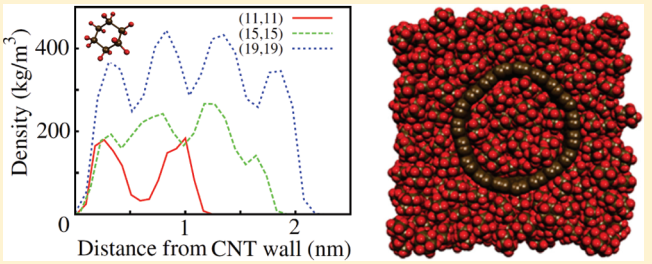

1. INTRODUCTION

Relaxation dynamics of electronic and vibrational excitations in carbon nanotubes (CNTs) have attracted significant experimental[1−7] and theoretical[8−12] attention due to unique physical and optical properties of these nanoscale materials. However, relatively little consideration has been given to the role the surrounding media in the relaxation processes.[13,14] Solvents confined inside CNTs can behave drastically different from bulk,[15−17] and interactions between CNTs and confined solvents occur in many applications. Examples include nanofluidic channels,[18,19] electrochemical devices[17,20] and drug delivery.[21−23]

Transfer of electronic and vibrational energy deposited into CNTs by visible and infrared radiation can initiate reactions inside tubes and reverse functionalization of the outer tube walls. In the former case, the vibrational energy transfer from the tube to the surrounding solvent must occur at a sufficient rate to provide energy to the encapsulated species. In the latter case, the energy transfer to the solvent should not be too fast, such that enough of it remains within the tube and is funneled to the bond between the tube and the functional group. The interior of CNTs provides a novel chemical reaction environment that can substantially lower the energy barrier for a variety of chemical transformations.[24] CNT heating by near-infrared radiation can be used to accelerate the diffusion of molecules inside the tube and release encapsulated drug molecules.[22,23] Functionalization of the outer tube wall can be used to tailor and control electronic transport,[25] increase CNT solubility,[26] and link a variety of small molecules[27] and DNA,[28−31] allowing for CNT purification and separation.[28]

The initial optical pulse excites electrons. They rapidly equilibrate at an effective electronic temperature that is much higher than room temperature.[1] Then, within tens to hundreds of femtoseconds, the electronic energy is deposited into the high-frequency vibrational

Special Issue: Shaul Mukamel Festschrift

Received: September 14, 2010
Revised: October 24, 2010
Published: November 17, 2010

modes of the CNTs.[1−3,8,9] Additional long-time components are present in the electronic relaxation of semiconducting CNTs. They are associated with the nonradiative and radiative lifetimes of the low energy excited electronic states.[3,4,10−12] The high-frequency phonons of CNTs equilibrate with low-frequency phonons within a picosecond.[5−7] The low-frequency phonons transfer the energy to the surrounding medium. In our previous work, we found that the vibrational energy exchange between CNTs and liquid water is complete within a few picoseconds, and that over half of the energy is exchanged on a subpicosecond time-scale.[14]

The current study is motivated by the fundamental interest in the effect of polarity of the surrounding medium on the CNT properties. The dependence of condensed phase processes on the medium is of central importance in a variety of fields, ranging from atmospheric, to material, and to biological sciences. For example, the solvent dependence of the vibrational relaxation dynamics and geminate-recombination of chlorine dioxide has been studied extensively in an effort to elucidate atmospheric photochemistry.[32−34] Environment has a considerable impact on CNT optical properties, affecting both exciton binding energy and transition energy.[35,36] An appropriately chosen medium increases CNT solubility and helps in CNT purification.[26,28] A number of practical applications of CNTs, such as high-capacitance electrochemical devices,[17,20] rely on nonaqueous environments.

In this paper, the vibrational energy transfer from CNTs to solvating acetonitrile and cyclohexane molecules is investigated. To extend our previous study of the vibrational energy transfer in polar, protic water and to represent a complete range of solvent properties, we chose to focus on polar, aprotic acetonitrile, and nonpolar cyclohexane. Water exhibits specific translational and rotational dynamics under spatial confinement.[15,16] In comparison, confined acetonitrile only exhibits specific rotational motions.[17] The interactions in cyclohexane are expected to be nonspecific. It is reasonable to expect that the part of the response due to solvent−solvent interactions should exhibit a strong dependence on solvent polarity.

The CNT and solvent models used for the simulations are presented in the next section, followed by a description of the calculation methods. A detailed analysis of the CNT-acetonitrile and CNT-cyclohexane vibrational energy exchange is provided in the Results and Discussion. Also in this section, we compare the current findings with the results from our previous study of the CNT-water system.[14] The key conclusions of this study are summarized in the final section of the paper.

2. THEORY

In this section, we first present the details of the molecular dynamics (MD) simulations, including a brief description of the force field models used to represent the CNTs, solvent molecules, and CNT-solvent interactions. Then, we describe the methods used for the data analysis.

2.1. Simulation Details. For each solvent, we performed classical MD simulations on three CNT-solvent systems containing single-walled armchair CNTs of different diameter. Specifically, the (11,11), (15,15), and (19,19) metallic armchair CNTs with corresponding diameters of 1.49, 2.03, and 2.58 nm were used.[37] Open-ended CNTs of 6.4 nm length were immersed in either liquid acetonitrile or liquid cyclohexane with the bulk densities of 776.8 and 779 kg/m^3, respectively, at 298 K. The

Table 1. CNT Details, Including Diameter, d, Outside and Inside Surface Area, SA_{out} and SA_{in}, and Volume, Vol_{in}

CNT	d, nm	SA_{out}, nm^2	SA_{in}, nm^2	Vol_{in}, nm^3
(11,11)	1.49	37.6	21.0	5.8
(15,15)	2.03	48.5	31.2	12.9
(19,19)	2.58	59.5	41.6	22.9

Table 2. Number of Solvent Molecules Outside, N_{out}, and Inside, N_{in}, of CNTs

acetonitrile	N_{in}	N_{out}
(11,11)	71	757
(15,15)	157	902
(19,19)	277	1046
cyclohexane	N_{in}	N_{out}
(11,11)	35	542
(15,15)	77	594
(19,19)	135	792

CNTs were centered in square parallelepiped simulation cells of the same length. To provide a good description of solvation, the systems were composed such that the solvent molecules surrounding the CNTs formed approximately two solvation shells.[33,38] Table 1 provides system details including diameter, inner and outer surface area, and the enclosed volume for each CNT. The number of solvent molecules inside and outside of each tube is listed in Table 2.

The GROMACS software package[39] was used to perform the MD simulations. The initialization step and data analysis were carried out using several proprietary utilities. The MD simulations were performed in the *NVT* ensemble using the Nose−Hoover thermostat[40] with a 0.1 ps relaxation time. For each system, 1000 ps data collection runs were generated following a 1000 ps equilibration period, and the MD time step of 1 fs was employed.

Acetonitrile molecules were treated using the three-site model,[41] and the methyl group was represented using the united-atom force field. Cyclohexane was constructed from carbon and hydrogen atoms according to the optimized potential for liquid simulations in the all-atom (OPLS-AA) force field, which explicitly contains every atom, including nonpolar hydrogens.[42] The CNT model used in the present simulation was developed by fitting the experimental lattice parameters, elastic constants and phonon frequencies for graphite, describing the interatomic potentials between sp^2 carbon centers.[43] The values of these parameters can be found in our previous work.[14] The effective diameter of a single carbon atom of the nanotube was estimated to be 0.38 nm based on the interatomic distance at the minimum of the pairwise interaction potential.[44] The system components and examples of solvated tubes are shown in Figure 1.

The sum of the Lennard-Jones (LJ) 12-6 and Coulomb potentials was used to describe the nonbonded site−site interactions between all atom pairs in the system

$$U(r_{ij}) = 4\varepsilon_{ij}\left[\left(\frac{\sigma_{ij}}{r_{ij}}\right)^{12} - \left(\frac{\sigma_{ij}}{r_{ij}}\right)^{6}\right] + \frac{z_i z_j e^2}{4\pi\varepsilon_0 r_{ij}} \qquad (1)$$

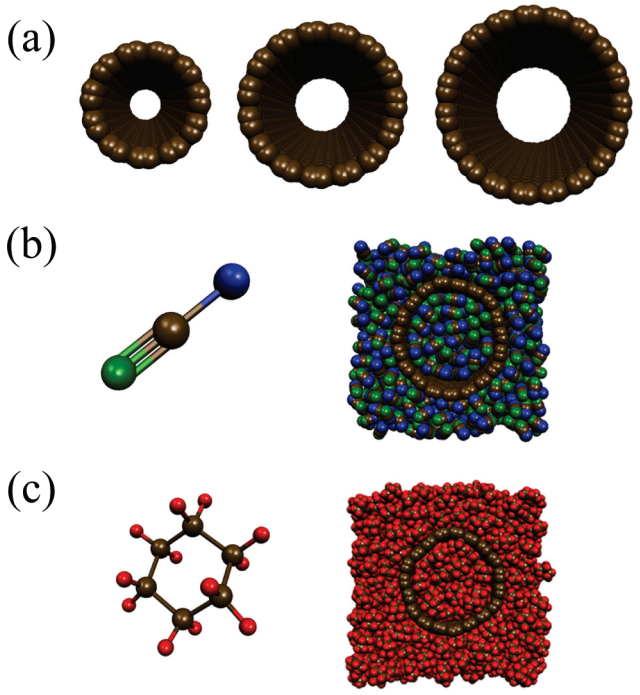

Figure 1. (a) (11,11), (15,15), and (19,19) CNTs used in the simulations. Side view of the square parallelepiped simulation cell for the (19,19) CNT with (b) acetonitrile and (c) cyclohexane. The solvent molecules outside the tubes comprise approximately two solvation shells. Brown, red, and green atoms represent carbon, hydrogen, and nitrogen, respectively. The methyl group is represented as a single blue atom to indicate the use of a united atom force field.

where ε_{ij} and σ_{ij} are the LJ parameters between sites i and j of distinct molecules, z_i is the partial charge on site i, and r_{ij} is the site−site separation. The Lorentz−Berthelot combining rules were used to obtain the cross interaction parameters

$$\varepsilon_{ij} = \sqrt{\varepsilon_{ii}\varepsilon_{jj}} \tag{2}$$

$$\sigma_{ij} = \frac{(\sigma_{ii} + \sigma_{jj})}{2} \tag{3}$$

A shifted force potential was employed for the LJ part of the potential, whereas the switch method was used to calculate the long-range Coulomb part.[45] The CNT-solvent interactions were treated as purely LJ, whereas the solvent−solvent interactions were treated with both LJ and Coulomb potentials.

2.2. Data Analysis. The basis for our analysis is derived from the linear response theory.[46−49] According to the theory, a nonequilibrium response of a system to a sufficiently small perturbation can be fully characterized by equilibrium fluctuations in the corresponding interaction energy. We consider the interactions between CNTs and solvent inside and outside the CNTs. These interactions characterize the rate of energy transfer from optically heated CNTs to the solvent, show whether the transfer differs for solvent inside and outside the tube, and indicate how rapidly the energy deposited into the solvent equilibrates between the inside and outside regions.

The normalized autocorrelation function (ACF) for the relevant interaction energy E is defined as

$$C(t) = \frac{\langle \Delta E(t)\Delta E(0)\rangle}{\langle \Delta E^2(0)\rangle} \tag{4}$$

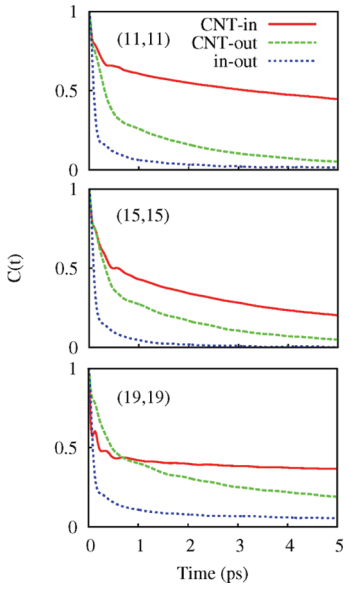

Figure 2. Normalized ACFs of the interaction energies for the (11,11), (15,15) and (19,19) CNTs in acetonitrile (top, middle, and bottom panels, respectively). The red (solid) and green (dashed) lines represent the interactions of the CNTs with the inside and outside solvent, respectively. The blue (dotted) line describes the Coulomb interaction between the solvent molecules inside and outside the CNTs.

where the brackets denote canonical ensemble averaging, and $\Delta E = E - \langle E\rangle$ indicates deviation of the interaction energy from its average value $\langle E\rangle$. The initial value

$$\tilde{C}(0) = \langle \Delta E^2(0)\rangle \tag{5}$$

of the unnormalized ACF

$$\tilde{C}(t) = \langle \Delta E(t)\Delta E(0)\rangle \tag{6}$$

gives the fluctuation in the interaction energy and quantifies the magnitude of the interaction.

The calculated ACFs showed biexponential decay and were well approximated by the following fitting function

$$f(t) = Ae^{-t/\tau_{\text{fast}}} + (1-A)e^{-t/\tau_{\text{slow}}} \tag{7}$$

Here, the first and second terms describe the fast and slow components of the vibrational energy exchange with time-scales τ_{fast} and τ_{slow}, respectively. The amplitude of the fast component is represented by A, and $1 - A$ gives the amplitude of the slow component.

The spectral density, calculated via cosine Fourier transform of the ACF, was computed for each interaction type and tube size

$$I(\omega) = \int_{-\infty}^{\infty} C(t)\cos(\omega t)\mathrm{d}t \tag{8}$$

The intensity I and frequency ω of the spectral density identify the vibrational motions that contribute to the energy exchange.

3. RESULTS AND DISCUSSION

The transfer of vibrational energy between CNTs and solvent molecules is characterized by the ACFs. Equation 4 is shown in Figure 2 for CNTs in acetonitrile and in Figure 3 for the case of cyclohexane. The time-scales of the energy exchange are determined from the corresponding ACFs for each tube size and interaction type. In particular, we consider the interaction between

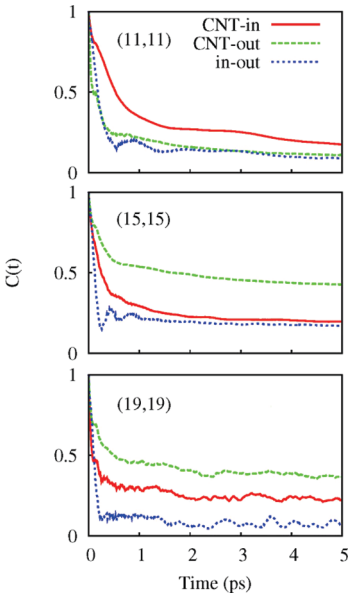

Figure 3. Same as Figure 2 for the CNTs in cyclohexane.

the CNT and solvent molecules inside the tube (CNT-in), the CNT and solvent molecules outside of the tube (CNT-out), and the interaction between solvent molecules inside the tube and solvent molecules surrounding the tube (in−out). The region outside the tube is represented by solvent molecules contained within the first two solvation shells around the tube. In most systems, the first two solvation shells are sufficient to account for the overwhelming part of the solvent response.[33,34,38] This observation should hold particularly well for CNTs, since they are neutral and apolar, and the CNT-solvent interactions are short-ranged.

The parameters for the biexponential fits, eq 7, of the ACFs from Figures 2 and 3 are presented in Table 3. The ACFs show fast and slow decay components arising from ballistic and diffusive relaxation mechanisms, respectively.[33,34,38] Ballistic relaxation results from direct pairwise collisions between the two subsystems, while collective motions within each subsystem are responsible for diffusive relaxation. In particular, in the present case the fast, ballistic component of the energy transfer can be described by the local interactions of the CNT with individual solvent molecules, neglecting the solvent−solvent interactions. In contrast, the slow, diffusive component is facilitated by long-range solvent−solvent interactions involving reorientation and collective displacements of solvent molecules, and by anharmonic coupling between CNT vibrational modes.

The CNT-solvent vibrational energy exchange exhibits the same general trends in acetonitrile and cyclohexane as in water.[14] This may be surprising at first, since water, acetonitrile, and cyclohexane have very different properties, as discussed in the Introduction. The similarity stems from the fact that the CNT-solvent interaction is dominated by the short-range LJ component, and thus, it is independent of the solvent polarity. The biggest differences in the CNT-solvent energy exchange for the three solvents are observed within the confined region. The behavior of the confined solvent does depend on molecular properties, such as polarity and hydrogen bonding.[15−17] Further, the structure of the confined solvent depends simultaneously on the CNT diameter and the size of the solvent molecules. The

Table 3. Time-Scales for ACFs, Equation 4, Obtained with Bi-Exponential Fitting, Equation 7, and the Initial Values of Unnormalized ACFs, Equation 6

acetonitrile	A_{fast}	τ_{fast}, ps	τ_{slow}, ps	$\tilde{C}$ (0), (kJ/mol)^2
CNT-In				
(11,11)	0.35	0.14	12.33	845
(15,15)	0.48	0.18	4.97	1947
(19,19)	0.56	0.06	22.96	1787
CNT-Out				
(11,11)	0.64	0.25	2.51	2241
(15,15)	0.61	0.23	2.36	2950
(19,19)	0.55	0.27	5.47	3012
In−Out				
(11,11)	0.89	0.11	1.82	75
(15,15)	0.88	0.11	1.06	97
(19,19)	0.86	0.10	4.41	110
cyclohexane	A_{fast}	τ_{fast}, ps	τ_{slow}, ps	$\tilde{C}$ (0), (kJ/mol)^2
CNT-In				
(11,11)	0.67	0.42	8.43	1466
(15,15)	0.71	0.22	10.32	1486
(19,19)	0.68	0.07	11.82	1930
CNT-Out				
(11,11)	0.74	0.10	4.69	1225
(15,15)	0.45	0.21	16.72	2293
(19,19)	0.53	0.15	17.22	2653
In−Out				
(11,11)	0.82	0.18	7.41	5.0
(15,15)	0.78	0.10	19.25	1.5
(19,19)	0.89	0.10	9.24	1.5

details of the solvent structure inside CNT, including the number of solvation shells, their rigidity, and so forth, influence the CNT-solvent energy exchange.

The fast part of the relaxation of the ACF for the CNT-solvent interaction energy occurs on a subpicosecond time-scale. In nearly all cases, over half of the vibrational energy dissipation is achieved on this time scale. Several picoseconds are required for the remainder of the relaxation process. Communication between the CNT and exterior solvent shows little variation with CNT diameter for both acetonitrile and cyclohexane. In contrast, the vibrational energy exchange between the CNT and interior solvent molecules is highly dependent on the tube size.

The time-scale of the vibrational energy exchange between CNTs and interior acetonitrile molecules shows anomalous dependence on the tube diameter. The vibrational energy exchange with the tube interior is dominated by the diffusive component, which has a larger amplitude than the fast component for the (11,11) and (15,15) CNTs. The situation is reversed for the largest (19,19) tube. This is in direct contrast to the trend observed in water in which the transfer to interior water molecules is dominated by ballistic relaxation.[14] In either case, the strong dependence of the observed time-scale on the CNT diameter is caused by the extent of spatial confinement effects on the solvent inside of the tubes.

For acetonitrile, the anomalous decay times can be rationalized by taking into account the reorientation times for acetonitrile confined inside of small diameter CNTs.[17] Because of the

dx.doi.org/10.1021/jp108776q |J. Phys. Chem. B 2011, 115, 5260–5267

differing geometry of confined acetonitrile, the solvent reorientation time is much faster for the (15,15) tube than for the (11,11) tube, resulting in a dramatic decrease in the diffusive relaxation component for the former tube compared to the latter. In the smaller (11,11) tube, the acetonitrile molecules are arranged in a cylindrical shell with additional string of molecules close to the CNT axis. The extra string of molecules pushes the shell molecules close to the CNT wall, impeding the orientation dynamics. The diameter of the (15,15) tube, while larger, is not large enough to accommodate another complete shell of acetonitrile molecules. In this arrangement, the acetonitrile molecules are located farther away from the tube wall, resulting in a relatively rapid reorientation time and faster diffusive component of the energy exchange. The internal radius of the (19,19) CNT is larger than the acetonitrile confinement distance of 0.70 nm,[17] leading to solvent properties that resemble bulk. Thus, the diffusive relaxation component slows down, as expected, due to the increase in the number of solvent molecules. While the enhanced rigidity of icelike water confined in smaller tubes[15,16] allows for greater coupling between water molecules and an increase in the energy transfer rate, no enhanced coupling is observed in acetonitrile due to lack of hydrogen bonding. On the contrary, confinement of acetonitrile reduces the ability to accommodate excess vibrational energy by inhibiting reorientation of solvent molecules. The fast component reveals the strength of the CNT-solvent coupling and also reflects the confined geometry. The (15,15) CNT generates a slow response due to the increased separation between the acetonitrile molecules and the tube wall, causing weaker coupling. The remaining tubes indicate stronger coupling.

In contrast to acetonitrile, the communication between CNTs and interior cyclohexane molecules is dominated by the fast component. The vibrational energy exchange is slow for narrow CNTs and speeds up for larger tubes. The ballistic component is accelerated in larger tubes, since they provide more space for the bulky cyclohexane molecule to move and accommodate the excess energy. The geometry of the confined cyclohexane system should play an important role in the solvent response; although to date, there has been no study of such confined cyclohexane systems. The diffusive solvent response is less significant due to the weak solvent−solvent interactions in cyclohexane. In this case, however, the weak solvent−solvent interactions lead to incomplete damping manifested as oscillations in the ACF, Figure 3; rather than transfer energy to neighboring solvent molecules, cyclohexane molecules transfer energy back to the CNT. Both fast and slow components of the ACF decay reflect this oscillatory exchange between solvent and CNT. For cyclohexane, the diffusive component of the CNT-inside interaction increases in proportion to the inner surface area of the tubes, Table 1.

For both acetonitrile and cyclohexane, the communication between the interior and exterior solvent subsystems is very fast and dominated by the ballistic component. However, the magnitude of this long-range Coulomb interaction is significantly weaker than that of the short-range LJ interaction between solvent and CNT, as evidenced by the magnitudes of the fluctuations in the interaction energy, eq 5, shown in the last column of Table 3. Any disbalance between the local temperatures of the inside and outside regions of the solvent will equilibrate through a tube-mediated interaction, rather than by a direct coupling between the two solvent subsystems. The solvent−tube interaction plays a greater role as the solvent

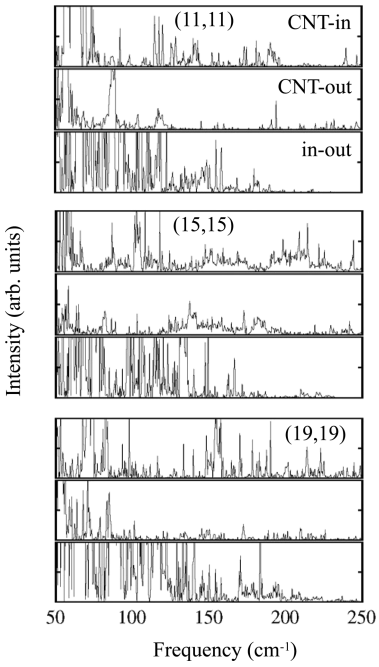

Figure 4. Spectral densities for the (11,11), (15,15), and (19,19) CNTs in acetonitrile (top, middle, and bottom panels, respectively). Each panel is divided into the CNT-inside, CNT-outside, and inside−outside data. The spectra are produced by Fourier transform of the ACFs, eq 8, and indicate the phonon modes responsible for the corresponding interaction. The same intensity range and frequency scale are used in all plots.

polarity decreases. The magnitude of the coupling between the interior and exterior acetonitrile molecules is smaller than for water, and the coupling for cyclohexane is even smaller. This is illustrated clearly by the decrease in the $\tilde{C}(0)$ values and increase in the diffusive decay time as the solvent polarity decreases, Table 3.

The CNT phonons that contribute to the relaxation are analyzed in Figures 4 and 5 for acetonitrile and cyclohexane, respectively. The spectral density, eq 8, is presented for each tube size and interaction type. While the intensity units are arbitrary, the intensity range and frequency scale are the same in all plots. In general, the vibrational energy exchange between CNTs and solvents is facilitated by low frequency modes below 100 cm^{-1}. The highest frequencies seen in the spectral densities correspond to the CNT radial breathing modes (RBM) and appear in the region from 100−250 cm^{-1}. Many types of local vibrational modes with frequencies higher than RBMs exist both in CNTs and solvents, however, the contribution of these local modes is insignificant. The changes in the RBM intensity with increasing tube size correlate with the changes in the relaxation time scales, indicating RBMs as a vital factor that determines the CNT-solvent vibrational energy exchange.

For the CNT-inside interaction in acetonitrile the RBM intensity grows as the tube size increases. The increase in the RBM intensity correlates with the faster ballistic decay time for larger tubes. For the same interaction in water, the disappearance of the RBM frequencies for larger tubes explains the slowing down of the transfer.[14] The decay times for the CNT-inside interaction in cyclohexane, which are slow for small tubes and faster for large tubes, can also be supported by the appearance of the RBM frequencies for larger tubes. Although less pronounced,

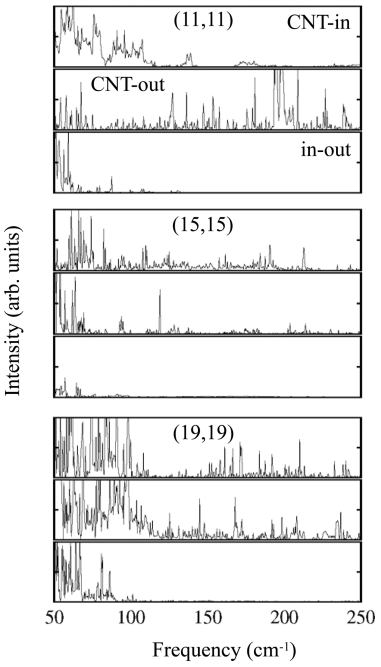

Figure 5. Same as Figure 4 for the CNTs in cyclohexane.

Table 4. CNT-Solvent Vibrational Energy Transfer Rates, *k*, Per Solvent Molecule

acetonitrile	k_{in}, ps^{-1}/molecule	k_{out}, ps^{-1}/molecule
(11,11)	0.100	0.0053
(15,15)	0.035	0.0048
(19,19)	0.060	0.0035
cyclohexane	k_{in}, ps^{-1}/molecule	k_{out}, ps^{-1}/molecule
(11,11)	0.068	0.018
(15,15)	0.059	0.008
(19,19)	0.106	0.008

the changes in the CNT-outside spectra can be correlated to changes in the decay rate as well. As expected, the inside−outside spectra remain relatively constant for different tube sizes in acetonitrile. The same spectra in cyclohexane reveal no signal in the RBM frequency range, Figure 5.

The fast, ballistic relaxation is well described by the binary collision model.[50] Therefore, the fast decay rate, $1/\tau_{fast}$, can be viewed as the sum of the rates due to individual solvent molecules, and any correlations between the molecules can be neglected. This fact allows us to define rigorously ballistic transfer rates per solvent molecule. Table 4 lists the transfer rates calculated per molecule for the CNT-inside and CNT-outside interactions. The data are plotted in Figures 6 and 7 for acetonitrile and cyclohexane, respectively. The bulk solvent that extends infinitely far away from the tube makes little contribution to the outside rates due to the short-range nature of the LJ interaction. Thus, the two solvation shells surrounding the CNTs in the present simulation cells are sufficient to account for the CNT-outside solvent interaction. This is supported by the fact that the CNT-outside transfer rate remains fairly constant with increasing CNT diameter for both acetonitrile and cyclohexane, as should be expected.

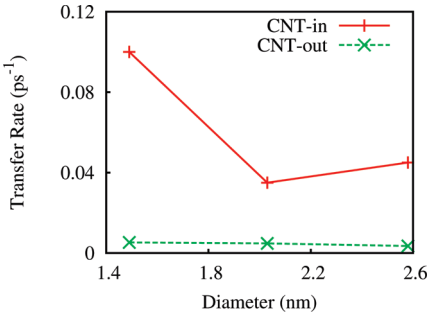

Figure 6. The rates of the CNT-acetonitrile vibrational energy transfer per molecule for the inside (solid red line) and outside (dashed green line) solvent, see Table 4.

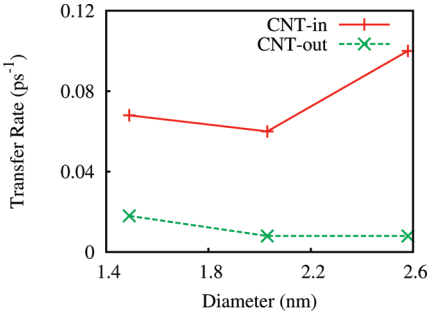

Figure 7. Same as Figure 6 for the CNTs in cyclohexane.

A larger tube has a greater radius of curvature than a smaller tube, causing the surface of larger tubes to appear increasingly planar at the molecular level. The rate of vibrational energy transfer from the CNT to the tube interior should decrease with increasing radius due to a decrease in the number of CNT-solvent interactions. Since the inner and outer tube surfaces both appear planar in the infinite size limit, the CNT-inside and CNT-outside rates should approach the same value. This trend was observed for CNTs in water.[14] The vibrational energy transfer rates per molecule to the inside and outside regions of the tube appear to diverge in both acetonitrile and cyclohexane, Figures 6 and 7. This fact indicates that the tube radii considered in the present study are too small in order to allow the confined solvent approach the bulk behavior. This is in contrast to water, for which the (19,19) CNT essentially gives the bulk limit.[14]

Figure 8 shows the density of cyclohexane confined within the (11,11), (15,15), and (19,19) CNTs. The plotted density values should be compared with the bulk density of 779 kg/m^3. Clearly, the bulk limit is not approached even with the largest tube. The cyclohexane structure inside the (11,11) CNT shows one distinct solvent layer. Similarly, there are two well-developed solvent layers inside the (19,19) CNT. The solvation structure of cyclohexane confined within the (15,15) CNT is not as well-defined. The peaks in the solvent density corresponding to individual solvent layers are not as sharp as for the (11,11) and (19,19) CNTs. The second layer starts to form; however, the fluctuations in the solvent structure are large, as indicated by the asymmetry in the density profile.

The anomalous behavior of acetonitrile, see ref 17 and cyclohexane, see Figure 8, confined inside the (15,15) CNT provide further rationalization for the apparent divergence of the data shown in Figures 6 and 7. In this solvent arrangement,

dx.doi.org/10.1021/jp108776q |J. Phys. Chem. B 2011, 115, 5260–5267

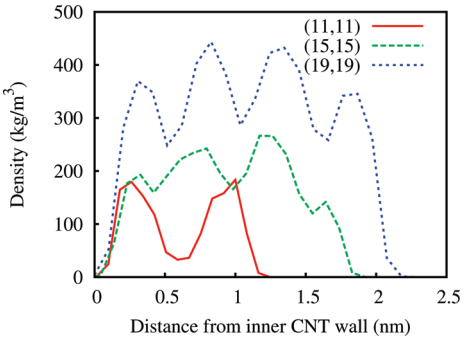

Figure 8. The density of cyclohexane confined inside the CNTs is plotted as a function of the distance from the inner CNT wall. The solid red line indicates the existence of a single cylindrical solvent shell inside the (11,11) tube. The dashed green line, corresponding to the (15,15) tube, reveals partial formation of a second solvation shell and an increase in solvent density. Finally, the dotted blue line indicates the presence of two distinct solvation shells inside the (19,19) tube and a marked increase in solvent density.

the distance between the CNT wall and the acetonitrile solvation shell is large resulting in a relatively weak CNT-acetonitrile coupling and an uncharacteristically small transfer rate. In cyclohexane, the CNT-inside transfer rate correlates with the density of the confined cyclohexane. The (11,11) and (15,15) tubes are in a low-density regime, while the (19,19) tube is in the high-density regime, Figure 8. We hypothesize that in the low-density regime, the distance between the CNT wall and the outermost solvent shell is the dominant factor in determining the transfer rate. The distance is larger for the (15,15) tube compared to the (11,11) tube; the increased separation in the (15,15) tube results in a weaker CNT-cyclohexane coupling and a decrease in the transfer rate. In the high-density regime, it is the number of tube-solvent interactions that determines the transfer rate. There is a marked increase in the transfer rate for the (19,19) tube compared to the (11,11) and (15,15) CNTs due to the higher density of solvent molecules near the CNT wall. As the tube wall becomes flatter, the number of CNT-solvent interactions decreases. Therefore, in the high-density regime the transfer rate per molecule will decrease with increasing CNT diameter and will approach the bulk limit.

4. DISCUSSION AND CONCLUSIONS

Using classical MD, we have investigated the rates and atomistic details of vibrational energy exchange between a series of CNTs and two nonaqueous solvents, acetonitrile and cyclohexane. Following our earlier studies of the CNT-water interactions, we have come to a relatively unexpected conclusion that the rates and mechanism of the energy transfer is generally independent of the solvent properties, even though the three solvents are very different. Water is polar, hydrogen bonding with a small molecular mass. Acetonitrile is polar, non-hydrogen bonding with a larger molecular mass. Cyclohexane is apolar, and its molecules are rather large and heavy, compared to water and acetonitrile. In all three cases, the exchange of vibrational energy between the CNTs and the solvents shows fast and slow time scales. In the majority of the systems, over half of the energy is transferred on the fast time scale in less than one picosecond, indicating that the dominant transfer mechanism is inertial relaxation produced by direct collisions of CNTs with individual solvent molecules. This relaxation mechanism rationalizes the weak solvent dependence of the energy exchange properties. The short-range nature of the CNT-solvent interaction represented by the LJ potential is responsible for the main relaxation pathway and is similar in all solvents. The long-range Coulomb interaction does differ between the solvents. However, its contribution to the overall relaxation is relatively small. The Coulomb interaction is important during the longer, diffusive relaxation stage that involves collective motions of the solvent molecules. The diffusive stage does show differences between the solvents. It requires from several picosecond to tens of picoseconds.

The differences between the three solvents become substantial for the energy exchange in the confined regime. This is because the extent of the confinement depends strongly on the molecular size. Within the same series of CNTs the CNT-water interaction approaches the bulk behavior, while the density of cyclohexane inside the largest CNT is barely half of the corresponding bulk value. In acetonitrile, the vibrational energy exchange with the tube interior is dominated by the diffusive component in the smaller CNTs, and only in the largest CNT the inertial component dominates. This is in direct contrast to water, in which the energy transfer to interior water molecules is dominated by inertial relaxation even in the smaller tubes. Generally, the confinement effects on the relaxation dynamics can be understood by considering the details of the solvent structure in the interior CNT region. In water, confinement can favor icelike structures that greatly affect all types of solvent dynamics. In acetonitrile, only rotational solvent motions are affected by the confinement, while translational diffusion exhibits uniform diameter dependence. The main effect seen with cyclohexane is the dramatic lowering of the solvent density inside small and medium size CNTs.

The communication between the interior and exterior solvent is fast but weak. It is facilitated by the long-range Coulomb interaction, whose strength rapidly drops from water, to acetonitrile, to cyclohexane. One can expect that direct communication between the two solvent subsystems is insignificant overall, and that the equilibration of the disbalance between the inside and outside solvent temperatures is mediated by the CNTs.

The current classical MD model of the CNT-solvent interaction ignores polarization of the CNTs by the solvents. This effect should be insignificant for cyclohexane, which is apolar; however, acetonitrile and especially water may significantly polarize the CNTs. This issue can be investigated by ab initio MD. However, it is extremely computationally demanding compared to classical MD. Alternatively, one can develop polarizable classical force-field models.[51,52] In present, these models are limited to few solvents and require extensive testing before reliable conclusions can be obtained.

The vibrational energy exchange between the CNTs and all three solvents is facilitated primarily by low frequency phonons within the energy range corresponding to CNT RBMs. These acoustic modes affect the cylindrical shape of the tubes and are strongly coupled to the solvent. The high frequency optical C−C stretching motions of the tubes have little effect on the CNT-solvent energy exchange.

The current study was largely motivated by the unique optical properties of CNTs. At the initial state, an optical pulse excites electrons, which rapidly transfer the energy to the optical modes of the tubes. The subsequent step involving the energy transfer from the optical modes to RBMs requires around a picosecond. The current study shows that, regardless of the nature of the

surrounding medium, a significant fraction of the RBM energy is deposited to the environment on a similar, picosecond time scale.[5−7] Even though one can clearly distinguish the three separate stages in the evolution of the optical energy deposited into CNTs, the last two stages involving energy transfer from C−C stretches to RBMs and from RBMs to solvent occur in parallel. Therefore, the theoretical predictions made in the current paper can be verified by performing the experiments of refs 5−7 in acetonitrile and cyclohexane. The similarity of the energy transfer between CNTs and three different solvents suggests that the conclusions of the present work should hold for CNTs kept in a polymer matrix[53] or wrapped by a DNA.[28,31]

AUTHOR INFORMATION

Corresponding Author

* E-mail: oleg.prezhdo@rochester.edu.

ACKNOWLEDGMENT

The work was supported by the NSF Grant CHE-1050405.

REFERENCES

(1) Hertel, T.; Moos, G. *Phys. Rev. Lett.* **2000**, *84*, 5002.
(2) Manzoni, C.; Gambetta, A.; Menna, E.; Meneghetti, M.; Lanzani, G.; Cerullo, G. *Phys. Rev. Lett.* **2005**, *94*, 207401.
(3) Carlson, L. J.; Krauss, T. D. *Acc. Chem. Res.* **2008**, *41*, 235.
(4) Hagen, A.; Steiner, M.; Raschke, M. B.; Lienau, C.; Hertel, T.; Qian, H. H.; Meixner, A. J.; Hartschuh, A. *Phys. Rev. Lett.* **2005**, *95*, 197401.
(5) Song, D. H.; Wang, F.; Dukovic, G.; Zheng, M.; Semke, E. D.; Brus, L. E.; Heinz, T. F. *Phys. Rev. Lett.* **2008**, *100*, 225503.
(6) Kang, K.; Ozel, T.; Cahill, D. G.; Shim, M. *Nano Lett.* **2008**, *8*, 4642.
(7) Luer, L.; Gadarmaier, C.; Crochet, J.; Hertel, T.; Brida, D.; Lanzani, G. *Phys. Rev. Lett.* **2009**, *102*, 127401.
(8) Habenicht, B. F.; Craig, C. F.; Prezhdo, O. V. *Phys. Rev. Lett.* **2006**, *96*, 187401.
(9) Habenicht, B. F.; Kamisaka, H.; Yamashita, K.; Prezhdo, O. V. *Nano Lett.* **2007**, *7*, 3260.
(10) Habenicht, B. F.; Prezhdo, O. V. *Phys. Rev. Lett.* **2008**, *100*, 197402.
(11) Perebeinos, V.; Avouris, P. *Phys. Rev. Lett.* **2008**, *101*, No. 057401.
(12) Kilina, S.; Badaeva, E.; Piryatinski, A.; Tretiak, S.; Saxena, A.; Bishop, A. R. *Phys. Chem. Chem. Phys.* **2009**, *11*, 4113.
(13) Rotkin, S. V.; Perebeinos, V.; Petrov, A. G.; Avouris, P. *Nano Lett.* **2009**, *9*, 1850.
(14) Nelson, T. R.; Chaban, V. V.; Kalugin, O. N.; Prezhdo, O. V. *J. Phys. Chem. B* **2010**, *114*, 4609.
(15) Hummer, G.; Rasaiah, J. C.; Noworyta, J. P. *Nature* **2001**, *414*, 188.
(16) Mashl, R. J.; Joseph, S.; Aluru, N. R.; Jakobssen, E. *Nano Lett.* **2003**, *3*, 589.
(17) Kalugin, O. N.; Chaban, V. V.; Loskutov, V. V.; Prezhdo, O. V. *Nano Lett.* **2008**, *8*, 2126.
(18) Xue, Y.; Chen, M. *Nanotechnology* **2006**, *17*, 5216.
(19) Whitby, M.; Quirke, N. *Nat. Nanotechnol.* **2007**, *2*, 87.
(20) Service, R. F. *Science* **2006**, *313*, 902.
(21) Bhirde, A. A.; Patel, V.; Gavard, J.; Zhang, G.; Sousa, A. A.; Masedunskas, A.; Leapman, R. D.; Weigert, R.; Gutkind, J. S.; Rusling, J. F. *ACS Nano* **2009**, *3*, 307.
(22) Hilder, T. A.; Hill, J. M. *Small* **2009**, *5*, 300.
(23) Chaban, V. V.; Savchenko, T. I.; Kovalenko, S. M.; Prezhdo, O. V. *J. Phys. Chem. B* **2010**, *114*, 13271.
(24) Halls, M. D.; Raghavachari, K. *Nano Lett.* **2005**, *5*, 1861.
(25) Zhao, Y. L.; Stoddart, J. F. *Acc. Chem. Res.* **2009**, *42*, 1161.
(26) Dyke, C. A.; Tour, J. M. *Chem.—Eur. J.* **2004**, *10*, 812.
(27) Campidelli, S.; Klumpp, C.; Bianco, A.; Prato, M. *J. Phys. Org. Chem.* **2006**, *19*, 531.
(28) Zheng, M.; Jagota, A.; Semke, E. D.; Diner, B. A.; Mclean, R. S.; Lustig, S. R.; Richardson, R. E.; Tassi, N. G. *Nat. Mater.* **2003**, *2*, 338.
(29) Yarotski, D. A.; Kilina, S. V.; Talin, A. A.; Tretiak, S.; Prezhdo, O. V.; Balatsky, A. V.; Taylor, A. J. *Nano Lett.* **2009**, *9*, 12.
(30) Nelson, T.; Zhang, B.; Prezhdo, O. V. *Nano Lett.* **2010**, *10*, 3237.
(31) Rotkin, S. V. *Annu. Rev. Phys. Chem.* **2010**, *61*, 241.
(32) Foster, C. E.; Barham, B. P.; Reid, P. J. *J. Chem. Phys.* **2001**, *114*, 8492.
(33) Brooksby, C.; Prezhdo, O. V.; Reid, P. J. *J. Chem. Phys.* **2003**, *119*, 9111.
(34) Gunnerson, K. N.; Brooksby, C.; Prezhdo, O. V.; Reid, P. J. *J. Chem. Phys.* **2007**, *127*, 164510.
(35) Lefebvre, J.; Finnie, P. *Nano Lett.* **2008**, *8*, 1890.
(36) Ando, T. *J. Phys. Soc. Jpn.* **2010**, *79*, No. 024706.
(37) Radovic, L. R.; Thrower, P. A. *Chemistry and Physics of Carbon*; Marcel Dekker, Inc.: New York, 2003; Vol. 28.
(38) Prezhdo, O. V.; Rossky, P. J. *J. Phys. Chem.* **1996**, *100*, 17094.
(39) Hess, B.; Kutzner, C.; Spoel, D. V. D.; Lindahl, R. *J. Chem. Theory Comput.* **2008**, *4*, 435.
(40) Nose, S. *J. Phys.: Condens. Matter* **1990**, *2*, 115.
(41) Mountain, R. D. *J. Chem. Phys.* **1997**, *107*, 3921.
(42) Jorgensen, W. L.; Maxwell, D. S.; Tirado-Rives, J. *J. Am. Chem. Soc.* **1996**, *118*, 11225.
(43) Guo, Y.; Karasawa, N.; Goddard, W. A. *Nature* **1991**, *351*, 464.
(44) Li, L. J.; Khlobystov, A. N.; Wiltshire, J. G.; Briggs, G. A. D.; Nicholas, R. J. *Nat. Mater.* **2005**, *4*, 481.
(45) Steinbach, P. J.; Brooks, B. R. *J. Comput. Chem.* **2004**, *15*, 667.
(46) Mukamel, S. *Principles of Nonlinear Optical Spectroscopy*; Oxford University Press: New York, 1995.
(47) Schwartz, B. J.; , R. P. J. *J. Chem. Phys.* **1994**, *101*, 6902.
(48) Prezhdo, O. V.; Rossky, P. J. *Phys. Rev. Lett.* **1998**, *81*, 5294.
(49) Bragg, A. E.; Cavanagh, M. C.; Schwartz, B. J. *Science* **2008**, *321*, 1817.
(50) Larsen, R. E.; Stratt, R. M. *J. Chem. Phys.* **1999**, *110*, 1036.
(51) Ren, P. Y.; Ponder, J. W. *J. Phys. Chem. B* **2003**, *107*, 5933.
(52) Fischer, R.; Richardi, J.; Fries, P. H.; Krienke, H. *J. Chem. Phys.* **2002**, *117*, 8467.
(53) Zhang, M.; Atkinson, K.; Baughman, R. *Science* **2004**, *306*, 1358.